Title
The roles of SDHAF2 and dicarboxylate in covalent flavinylation of SDHA, the human complex II flavoprotein

Journal
Proceedings of the National Academy of Sciences of the United States of America, 117(38)

ISSN
0027-8424

Authors
Sharma, Pankaj
Maklashina, Elena
Cecchini, Gary
et al.

Publication Date
2020-09-22

DOI
10.1073/pnas.2007391117

Peer reviewed

The roles of SDHAF2 and dicarboxylate in covalent flavinylation of SDHA, the human complex II flavoprotein

Pankaj Sharma[a], Elena Maklashina[b,c], Gary Cecchini[b,c,1], and T. M. Iverson[a,d,e,f,1]

[a]Department of Pharmacology, Vanderbilt University, Nashville, TN 37232; [b]Molecular Biology Division, San Francisco Veterans Affairs Health Care System, San Francisco, CA 94121; [c]Department of Biochemistry and Biophysics, University of California, San Francisco, CA 94158; [d]Department of Biochemistry, Vanderbilt University, Nashville, TN 37232; [e]Center for Structural Biology, Vanderbilt University, Nashville, TN 37232; and [f]Vanderbilt Institute of Chemical Biology, Vanderbilt University, Nashville, TN 37232

Edited by Amy C. Rosenzweig, Northwestern University, Evanston, IL, and approved August 1, 2020 (received for review April 17, 2020)

Mitochondrial complex II, also known as succinate dehydrogenase (SDH), is an integral-membrane heterotetramer (SDHABCD) that links two essential energy-producing processes, the tricarboxylic acid (TCA) cycle and oxidative phosphorylation. A significant amount of information is available on the structure and function of mature complex II from a range of organisms. However, there is a gap in our understanding of how the enzyme assembles into a functional complex, and disease-associated complex II insufficiency may result from incorrect function of the mature enzyme or from assembly defects. Here, we investigate the assembly of human complex II by combining a biochemical reconstructionist approach with structural studies. We report an X-ray structure of human SDHA and its dedicated assembly factor SDHAF2. Importantly, we also identify a small molecule dicarboxylate that acts as an essential cofactor in this process and works in synergy with SDHAF2 to properly orient the flavin and capping domains of SDHA. This reorganizes the active site, which is located at the interface of these domains, and adjusts the pK_a of $SDHA^{R451}$ so that covalent attachment of the flavin adenine dinucleotide (FAD) cofactor is supported. We analyze the impact of disease-associated SDHA mutations on assembly and identify four distinct conformational forms of the complex II flavoprotein that we assign to roles in assembly and catalysis.

bioenergetics | complex II | protein folding | flavinylation | assembly

Respiratory complex II, also called succinate:quinone oxidoreductase, is a heterotetrameric, integral-membrane complex composed of the SDHA, SDHB, SDHC, and SDHD subunits (1–4). Complex II enzymes act in aerobic respiration; however, some facultative anaerobes contain a second homolog (FrdABCD) that acts during anaerobic respiration with fumarate (5, 6). Complex II supports bidirectional succinate-fumarate interconversion at a covalently-linked flavin adenine dinucleotide (FAD) within the flavoprotein subunit (SDHA) and links the tricarboxylic acid (TCA) cycle with quinol-quinone interconversion as part of respiration. In humans, missense mutations in the *SDHA* gene are associated with severe disease phenotypes, including Leigh syndrome, optic atrophy, and both benign and malignant paraganglioma tumors (7, 8).

Four identified assembly factors, termed SDHAF1, SDHAF2, SDHAF3, and SDHAF4, are dedicated to complex II assembly and maturation in humans (9–11). The roles of these assembly factors are not yet fully understood but may include: 1) assisting with cofactor insertion; 2) tuning the chemical reactivity of isolated subunits; 3) stabilizing isolated subunits during assembly; and/or 4) bringing together unassembled subunits (10–14). Patients with mutations in the SDHAF1, SDHAF2, or SDHAF3 complex II assembly factors can exhibit complex II insufficiency without having mutations in the complex II structural genes (9, 15–18). While there are currently no known disease-associated SDHAF4 mutations, studies in *Drosophila* suggest that alteration of this assembly factor impacts physiology of the organism (11). It has also been suggested that a stable human assembly intermediate, termed CII_{low}, contains SDHA and either SDHAF2 or SDHAF4. CII_{low} might have additional metabolic signaling functions during periods of bioenergetic stress (19).

Perhaps surprisingly, only SDHAF2 is conserved across all three kingdoms, where it is also called SdhE (bacteria, ref. 20) or Sdh5 (yeast, ref. 9). Based upon studies of these homologs, the function of SDHAF2 and its counterparts in complex II maturation is proposed as an assembly chaperone dedicated to maturation of the flavoprotein, (SDHA in mammals, Sdh1 in yeast, and SdhA/FrdA in bacteria). Specifically, SDHAF2 homologs have been shown to enhance covalent flavinylation, which is a requirement for the succinate oxidation reaction (9, 21). In the human SDHA protein, covalent flavinylation to the isoalloxazine ring of the FAD is through a C(8)-methyl-histidyl^{99}(*N*)ε-covalent bond.

Crystal structures of the *Escherichia coli* FrdA-SdhE (22) and SdhA-SdhE (23) assembly intermediates have been reported. In these structures, the core fold of SdhA/FrdA as well as SdhE were similar, with an rmsd of <1.0 Å for isolated domains of the flavoprotein or SdhE in pairwise alignments. Both studies identified that SdhE forms a hydrogen bond with the destination histidine ligand of the flavin ($FrdA^{H44}$/$SdhA^{H45}$, equivalent to $SDHA^{H99}$) and stabilizes the side chain in an orientation primed for covalent attachment. Both studies also indicated that this

Significance

Complex II is a membrane-spanning machine that supports respiration in all kingdoms. Complex II insufficiency can result from mutations in any of the genes encoding its subunits or from incorrect assembly. Here, we evaluate how a small molecule dicarboxylate works in synergy with the SDHAF2 assembly factor to promote covalent attachment of FAD to the SDHA subunit. We determine the structure of the human SDHA-SDHAF2 assembly intermediate with the dicarboxylate oxaloacetate and reveal how this pose contributes to complex II maturation. Our findings provide the structure of a part of human complex II and identify how SDHAF2 and the dicarboxylate organize the active site. Comparison to previous work reveals that multiple catalytic states change the active site parameters.

Author contributions: P.S., E.M., G.C., and T.M.I. designed research; P.S. and E.M. performed research; P.S., E.M., G.C., and T.M.I. analyzed data; and P.S., E.M., G.C., and T.M.I. wrote the paper.

The authors declare no competing interest.

This article is a PNAS Direct Submission.

[1]To whom correspondence may be addressed. Email: gary.cecchini@ucsf.edu or tina.iverson@vanderbilt.edu.

This article contains supporting information online at https://www.pnas.org/lookup/suppl/doi:10.1073/pnas.2007391117/-/DCSupplemental.

First published September 4, 2020.

assembly intermediate is associated with an altered active site architecture. The active site contains two histidines (human $SDHA^{H296}$, $SDHA^{H407}$), two arginines ($SDHA^{R340}$, $SDHA^{R451}$), and one threonine ($SDHA^{T308}$) (see *Footnote* and *SI Appendix*, Table S1) and is located at an interdomain interface. An interdomain rotation of the assembly intermediates appears to cause the altered alignment of these active site residues (22, 23). This prompted the structural prediction that the active site can no longer catalyze succinate-fumarate interconversion in this pose, which was consistent with kinetic analysis of the assembly intermediate, which lacks detectable succinate-fumarate interconversion activity (24). Despite the similarities in these two structures, the magnitude and the direction of this interdomain rotation was substantially different, creating controversy as to which of these accurately captured an on-pathway pose in the assembly process.

Sequence similarity suggests that the human SDHAF2 likely performs similar functions as the homologous bacterial SdhE; however, SDHAF2 is ∼50% larger, hinting at additional complexity during the maturation of the mitochondrial complex II flavoprotein. Here, we apply a biochemical reductionist approach to the maturation of human SDHA as assisted by small molecule dicarboxylates and the SDHAF2 assembly factor. We combine this with structural approaches to identify the route of maturation for the human complex II flavoprotein and show that the additional sequence regions unique to mitochondrial SDHAF2 are important for function. Our results provide insight into the essential role that dicarboxylate plays in the flavinylation reaction. In addition, we define the active site side chains required for flavinylation and predict how disease-associated SDHA mutations affect this assembly complex. Finally we propose how different poses of the assembly intermediates captured to date could represent different biological states of assembly.

Results

Reconstitution of SDHA Maturation In Vitro. Although it is believed that SDHAF2 is necessary for SDHA maturation, prior classic reconstructionist approaches to in vitro SDHA maturation have only been partially successful. In vitro SDHAF2-dependent flavinylation of SDHA in the presence of a dicarboxylate was previously shown by Zafreen et al. (25), although progress was hampered by both the instability of SDHA and the poor expression levels of SDHA. Toward the overall goal of in vitro flavinylation, prior work from us and others improved expression levels of SDHA using codon optimization (24), but the expression of functional and assembled human complex II continues to elude the field. This suggests that, to date, all components needed for human SDHA maturation and flavinylation have not been correctly defined.

Reconstruction of human SDHA maturation has been slightly more successful in *E. coli*. In past work, when human SDHA is heterologously expressed in *E. coli*, the apoprotein accumulated (recapitulated in Fig. 1*A*, lane 2 and *SI Appendix*, Fig. S1*A*) (24, 25), indicating that the *E. coli* machinery that supports complex II maturation cannot assemble the human counterpart. However, coexpression of SDHA with human SDHAF2 rescued correctly flavinylated SDHA (recapitulated in Fig. 1 *A* and *B* and *SI Appendix*, Fig. S1*A*), albeit in an intermediate form where SDHAF2 remained tightly bound to SDHA (*SI Appendix*, Fig. S1*B*). Following purification, the SDHA-SDHAF2 complex required denaturants to release the correctly flavinylated SDHA subunit (24). This requirement for a chaotropic agent or SDS (sodium dodecyl sulfate) to disassociate the SDHA-SDHAF2 assembly intermediate has parallels to historic studies that showed that the bovine SDHAB complex required trichloroacetic acid or perchlorate to disassociate (26), which reflects the SDHA-SDHB interface being stable in the cell. In fact, this SDHA-SDHAF2 intermediate is so stable that an affinity value cannot be measured in our hands. This level of binding strength is consistent with the SDHA-SDHAF2 complex being stable in the cell for long periods of time. In comparison, the homologous bacterial FrdA-SdhE complex readily dissociates, with a measured IC_{50} of 1.2 to 1.5 μM (22).

In order to reconstruct human SDHA maturation in vitro, we evaluated previous studies that indicated that small molecule dicarboxylates enhanced covalent FAD attachment (27, 28). Dicarboxylates include succinate and fumarate, which are the substrate and product of assembled mitochondrial complex II, respectively. Dicarboxylates also represent a range of off-pathway substrates or inhibitors that may regulate the TCA cycle via a feedback mechanism. We selected a range of biologically relevant dicarboxyates and found that all of these except citrate stimulated flavinylation above the negative control to some extent (Fig. 1 *A* and *B*, lane 8). The addition of succinate, fumarate, or malate to the in vitro reaction of purified *apo*-SDHA, SDHAF2, and FAD resulted in particularly robust covalent flavinylation of the SDHA subunit (Fig. 1 *A* and *B* and *SI Appendix*, Fig. S1*B*). Oxaloacetate, malonate, pyruvate, and L-aspartate stimulated SDHAF2-dependent flavinylation to a lesser extent (Fig. 1 *A* and *B*, lanes 6 and 7 and 9 and 10).

Kinetic analysis using the substrate and product of complex II, succinate and fumarate, showed a similar concentration requirement, with half-maximal flavinylation at 22 ± 2 μM and 16 ± 2 μM for succinate and fumarate, respectively (*SI Appendix*, Fig. S1*C*).

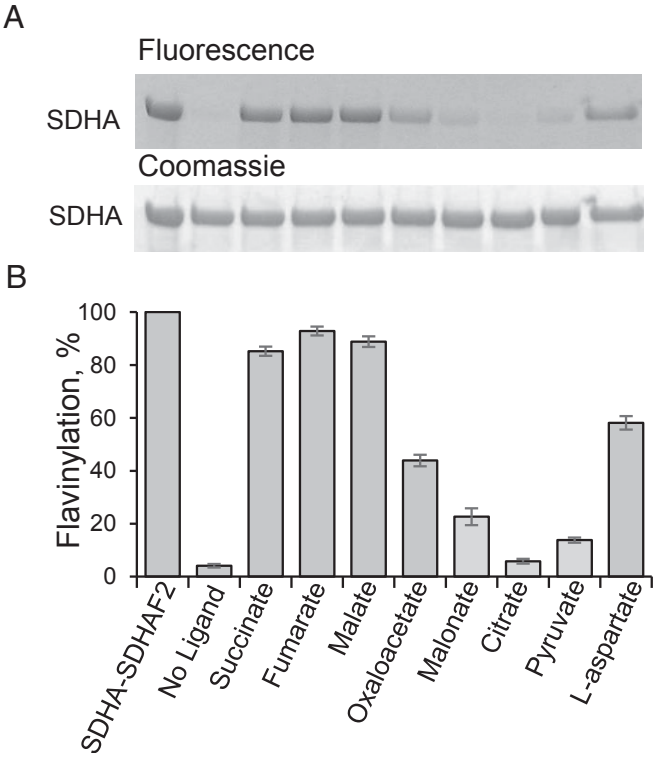

Fig. 1. In vitro flavinylation of apo-SDHA in the presence of SDHAF2. (*A*) Ligands promote SDHAF2-dependent flavinylation of apo-SDHA. Apo-SDHA (0.22 mg/mL) was incubated with SDHAF2 (0.08 mg/mL), 100 μM FAD, and 20 mM ligands in 50 mM Hepes pH 7.5 for 40 min at 37 °C. Lane 1, Holo-human SDHA isolated from *E. coli* when SDHA was coexpressed with SDHAF2, this lane is used as a 100% control. In-gel fluorescence of FAD-SDHA is shown at the *Top* and the amount of protein loaded per lane (Coomassie) is shown at *Bottom*. (*B*) Histogram representing the fluorescence intensity. Holo-SDHA-SDHAF2 (lane 1) was used as 100% flavinylation control. Error bars represents means ± SEM, $n = 4$ biological replicates. Statistical significance was assessed using a Student's t test in pairwise comparisons to the negative control. $P < 0.001$ for all samples except citrate ($P = 0.052$).

For FAD, half maximal flavinylation was achieved at 1.5 ± 0.3 μM FAD (*SI Appendix*, Fig. S1*D*). As measured by following the rate of covalent incorporation into apo-SDHA the observed rate of the SDHAF2-assisted flavinylation reaction, $k = 0.15 \pm 0.01$ min^{-1} (*SI Appendix*, Fig. S1*E*), corresponds well to other self-catalytic flavinylation reactions (29, 30). Thus, the minimally defined in vitro flavinylation reaction of apo-SDHA requires FAD, SDHAF2, and an appropriate dicarboxylate.

Unique Structural Features of the Human SDHA-SDHAF2 Assembly Intermediate. The mitochondrial signaling sequence of SDHAF2 corresponds to the first 37 amino acids (12). Using a construct of SDHAF2 lacking the first 30 amino acids, i.e., retaining 7 amino acids of the signal sequence, we performed crystallization trials of the human SDHA-SDHAF2 assembly intermediate in the presence of fumarate, succinate, malate, or oxaloacetate. We were only able to grow diffraction-quality crystals in the presence of oxaloacetate and used these crystals to determine the 2.6-Å resolution crystal structure of the human SDHA-SDHAF2 assembly intermediate (Fig. 2*A* and *SI Appendix*, Table S2) (31, 32). There are two complexes in each asymmetric unit. Both adopt a similar conformation and are consistent with SAXS (small angle X-ray scattering) spectroscopy of the purified complex (*SI Appendix*, Fig. S2). As a result, the numeric analyses here describe the A chain and its associated SDHAF2 assembly factor. In this structure, SDHA is covalently flavinylated such that the structure represents a product of the flavinylation reaction (Fig. 2*B*).

The first notable feature of the human SDHA-SDHAF2 complex is a hydrogen bond between SDHAF2^{G78} and SDHA^{H99}, the covalent ligand to the FAD (Fig. 2*B*). In the bacterial homologs, the equivalent interaction was proposed to stabilize and orient the histidine ligand for covalent flavinylation (22, 23). Consistent with this proposal is the finding that SDHAF2^{G78R} mutations in patients result in paragangliomas associated with complex II insufficiency (*SI Appendix*, Fig. S3 and Table S2) (9).

The observed stability of the human SDHA-SDHAF2 assembly intermediate may stem from the buried surface area, which is 1,922 Å^2. In the human SDHA-SDHAF2 interface,1,257 Å^2 of buried surface results from an interaction between the conserved five-helix bundle of SDHAF2 and SDHA, which is similar to the total buried surface area of the equivalent bacterial intermediates. For comparison, the *E. coli* FrdA-SdhE buries 1,072 Å^2 and required a cross-linker for stabilization while the *E. coli* SdhA-SdhE buried 1,458 Å^2 (Fig. 2*C* and *SI Appendix*, Table S4) (22, 23). The additional buried surface in the human SDHA-SDHAF2 assembly intermediate is via 14 N-terminal and 10 C-terminal amino acid residues that are part of the sequence extensions unique to the mitochondrial homologs (Fig. 2*D* and *SI Appendix*, Fig. S4 *A* and *B*). Curiously, these ordered termini are associated with little secondary structure (Fig. 2*D* and *SI Appendix*, Fig. S4*B*). As a result, these are intrinsically disordered regions if not bound to SDHA, as demonstrated by NMR spectroscopy of the yeast ortholog (33) (*SI Appendix*, Fig. S4*C*).

To test whether these unusual termini are important for the function of SDHAF2, we performed truncation mutagenesis

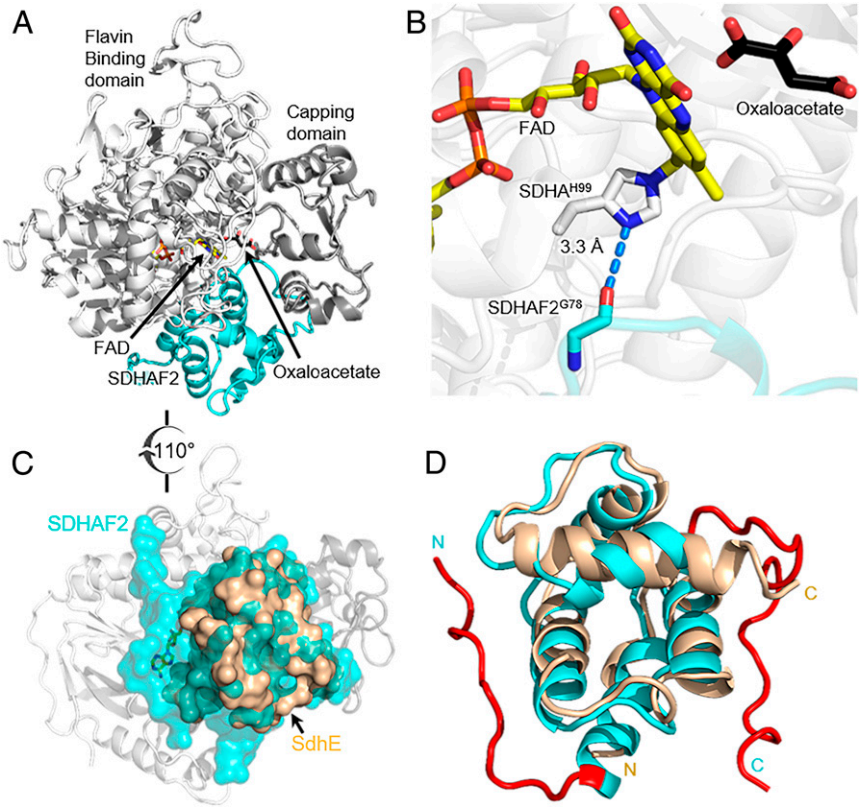

Fig. 2. Structure of human SDHA-SDHAF2 assembly intermediate. (*A*) The SDHA-SDHAF2 assembly intermediate in cartoon representation with the flavin-binding domain in white, the capping domain in gray, and SDHAF2 in cyan. The ligands are shown as sticks with the carbon atoms of the FAD in yellow and the carbon atoms of the oxaloacetate in black. (*B*) The hydrogen bond between SDHA^{H99} and SDHAF2^{G78}. SDHA^{H99} is the covalent ligand to FAD and this interaction is proposed to stabilize the orientation of this side chain during the flavinylation reaction. (*C*) Surface representation of SDHAF2 (cyan) superimposed with the *E. coli* homolog SdhE (wheat) from the FrdA-SdhE assembly intermediate (PDB ID 6B58) (22) illustrates the significantly larger interaction surface of SDHAF2 resulting from the extended N and C termini. The view is rotated 90° with respect to *A*. (*D*) Overlay of human SDHAF2 with *E. coli* SdhE (PDB ID 6B58) (22) highlights the extended N and C termini (red) of SDHAF2 and illustrates that these lack appreciable secondary structure.

(*SI Appendix*, Fig. S5*A*) and monitored covalent flavinylation of SDHA expressed in *E. coli*. We found that deletion of the 15 N-terminal amino acids upstream of the conserved five-helix bundle or the 15 C-terminal residues of SDHAF2 resulted in loss of robust binding to SDHA (*SI Appendix*, Fig. S5*B*), and these truncated proteins no longer facilitated SDHA flavinylation. This is somewhat surprising because the truncated SDHAF2 variants express well, are stable and unproteolyzed (*SI Appendix*, Fig. S5 *C* and *D*), and contain all regions found to be necessary for function in bacterial homologs (*SI Appendix*, Fig. S4*A*).

When compared to the mature and assembled porcine SDHA subunit (99% identical to human complex II; PDB ID 3SFD) (34), the human SDHA subunit in this assembly intermediate has a major difference in interdomain orientation resulting from SDHAF2 binding (Fig. 3*A*). In short, SDHAF2 binds to a site on SDHA that overlaps with the location where SDHB would bind in assembled porcine complex II (Fig. 3*B* and *SI Appendix*, Fig. S6 *A* and *B*). SDHAF2 is wedged between the two domains of SDHA: the flavin binding and the capping domain (Figs. 2*A* and 3*B*). Domain movement analysis using the Dyndom program (35) calculated that capping domain is rotated 25° as compared to its position in assembled porcine complex II (34) (Fig. 3 *A* and *C*). Notably, the bound dicarboxylate oxaloacetate is in a distinct orientation in the assembly intermediate as compared to mature complex II (34) (Fig. 3*D*) and this dicarboxylate appears to have a role in stabilizing the interdomain orientation.

Comparison of the SDHA-SDHAF2 intermediate to assembled complex II, the *E. coli* SdhA-SdhE complex crystallized in the absence of a dicarboxylate (*SI Appendix*, Fig. S6*C*) (23) and the *E. coli* FrdA-SdhE intermediate crystallized with malonate (*SI Appendix*, Fig. S6*D*) (22) highlights how the dicarboxylate stabilizes the domains. As compared to mature and assembled porcine complex II (34), where the two domains have numerous direct contacts, in the SDHA-SDHAF2 assembly intermediate, a disproportionate number of the interdomain interactions are instead mediated by the dicarboxylate (*SI Appendix*, Fig. S7 *A–D* and Tables S5 and S6). Specifically, the capping domain position is stabilized by 5 intraprotein hydrogen bonds, and 5 bonds through the dicarboxylate (*SI Appendix*, Fig. S7 *A* and *B* and Tables S5 and S6). This contrasts with the 15 intraprotein hydrogen bonds in the mature porcine complex II structure (34) (*SI Appendix*, Tables S5 and S6). Of particular interest is a salt bridge between the $SDHA^{D341}$ on the capping domain and $SDHA^{R662}$ on the flavin-binding domain and near the C terminus of SDHA of mature complex II (*SI Appendix*, Fig. S8*A*). Mutagenesis studies in complex II homologs have demonstrated that substitution or deletion of the residue equivalent to $SDHA^{R662}$ in yeast Sdh1 (36) or to $SDHA^{D341}$ in *E. coli* FrdA (37) inhibits flavinylation in those homologs. The SDHA-SDHAF2 structure identifies that these distal side chains stabilize the flavinylation-competent conformation of SDHA (*SI Appendix*, Fig. S8 *A* and *B*) consistent with previous speculations (14). Additional details of the differences in interdomain hydrogen bonding that accompany capping domain

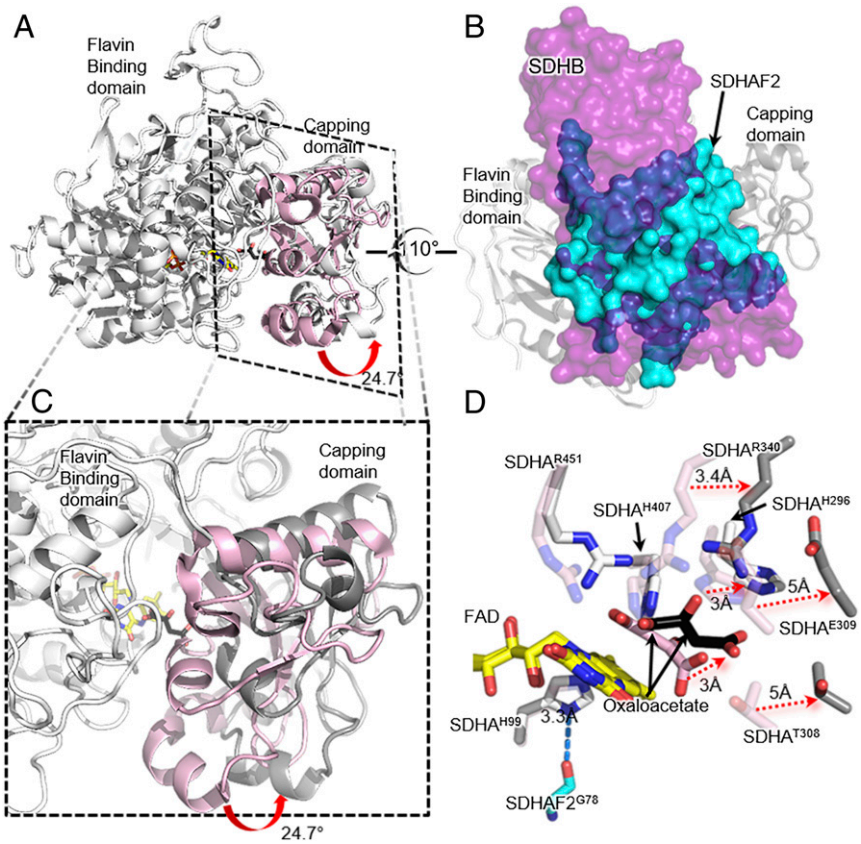

Fig. 3. Effect of SDHAF2 and dicarboxylate on the structure of the SDHA subunit. (*A*) Overlay of the flavin-binding domains of the SDHA subunit from the human SDHA-SDHAF2 assembly intermediate (white) and the assembled porcine complex II (light pink) (PDB ID 3SFD) (34) highlights a capping domain rotation of 24.7° (35). (*B*) Comparison of the human SDHA-SDHAF2 assembly intermediate to assembled porcine complex II (PDB ID 3SFD) (34) shows that human SDHAF2 (cyan surface) and porcine SDHB (magenta surface) use the same binding site on SDHA. (*C*) A closeup view comparing the capping domain position in assembled porcine SDHA (PDB ID 3SFD) (34) and human SDHA from the SDHA-SDHAF2 assembly intermediate. (*D*) FAD-based superposition of the SDHA active site from the SDHA-SDHAF2 assembly intermediate (white) and assembled porcine complex II (PDB ID 3SFD) (34) highlights the displacement of key active site residues in the assembly intermediate, which is predicted to disfavor the succinate-fumarate interconversion reaction.

rotation in the SDHA-SDHAF2 assembly intermediate are found in *SI Appendix*, Tables S5 and S6.

The altered position of the capping domain is important because the complex II active site is located at the interdomain interface and requires residues from both domains (Fig. 3*D*). Thus, a change in interdomain angle means that the geometry of enzymatically potent side chains differs. Rotation of the capping domain of SDHA by ~25° results in a shift of active site residues $SDHA^{H296}$, $SDHA^{R340}$, and $SDHA^{T308}$ by 3.0 Å, 3.4 Å, and 5 Å, respectively, compared to their position in porcine complex II (Fig. 3*D*).

Defining the Catalytic Residues for Covalent Flavinylation. Bacterial FrdA/SdhA have been used as model systems to study flavinylation, and six amino acids have been identified where mutation results in significant loss of covalent FAD (37, 38). Four of these are active site residues implicated in succinate-fumarate interconversion and are analogous to $SDHA^{H296}$, $SDHA^{H407}$, $SDHA^{R340}$, and $SDHA^{R451}$ (*SI Appendix*, Table S1). However, mutation of an active site threonine (equivalent to $SDHA^{T308}$) had no detectable effect on covalent flavinylation (39) (*SI Appendix*, Table S1). Further, residues equivalent to $SDHA^{E309}$ and $SDHA^{D341}$ are identified as being important for flavinylation but have not been assigned roles in succinate-fumarate interconversion (37). Thus, while there is overlap in the residues that are critical for flavinylation and succinate-fumarate interconversion, there are side chains that appear unique to each chemical reaction.

In the SHDA-SDHAF2 structure, $SDHA^{H296}$, $SDHA^{H407}$, $SDHA^{R340}$, and $SDHA^{R451}$ interact with oxaloacetate (Fig. 3), suggesting that that one role of these side chains in covalent flavinylation is to bind to the dicarboxylate cofactor. $SDHA^{R451}$ has been proposed to have an additional key role in that it localizes a positive charge above the FAD (22, 37, 40) in order to counterbalance the negative charge that develops in the N1/C2 region during the formation of the iminoquinone methide intermediate (41, 42) (*SI Appendix*, Fig. S9).

We propose that the two residues that are found outside of the active site, equivalent to $SDHA^{E309}$ and $SDHA^{D341}$ play supporting roles. The amide nitrogen of $SDHA^{E309}$ hydrogen bonds to the dicarboxylate cofactor and in one of the two molecules of the asymmetric unit, the $SDHA^{E309}$ side chain forms an interaction with $SDHA^{R340}$ that is unique to the assembly intermediate. This stabilizes the position of the $SDHA^{R340}$ so that it can bind dicarboxylate in the flavinylation orientation. $SDHA^{D341}$ forms a hydrogen-bonding interaction that appears to stabilize the position of the capping domain. Taken together, all of the identified side chains that eliminate flavinylation upon mutation (37) help to orient the dicarboxylate cofactor, stabilize the altered capping domain position, or both, while $SDHA^{R451}$ additionally stabilizes the transition intermediate.

Interestingly, the rotated position of the capping domain exposes the active site to solvent (*SI Appendix*, Fig. S10*A*). Ready access of solvent to the active site was previously reported in the structures of both bacterial assembly intermediates (22, 23, 43) (*SI Appendix*, Fig. S10*B*) where it instead involved unfolding of the polypeptide adjacent to the active site to form a defined tunnel (22, 23). However, a biological rationale for solvent access to the active site during flavinylation has not previously been proposed.

We considered whether there could be a chemical reason why solvent access would favor formation of the covalent bond to FAD and focused on $SDHA^{R451}$ because it stabilizes the intermediate. A major impact of the folded protein environment is that it can shift the pK_a values of the ionizable side chains and affect the charge. Because the side chain charge of $SDHA^{R451}$ is important for flavinylation, we calculated the pK_a of side chains equivalent to $SDHA^{R451}$ in assembled complex IIs (34, 44–46) as well as the human and bacterial assembly intermediates (22, 23) (*SI Appendix*, Table S7). In assembled complex IIs, this arginine is buried and the calculated pK_a of the side chain is between 4.4 and 8.0 in all but the *E. coli* FrdABCD structure, where it is 10, possibly because the active site in this structure is more open and contains additional hydration (46, 47). In contrast, in both the human SDHA-SDHAF2 structure and the two *E. coli* assembly intermediates (22, 23), the solvent exposure results in the calculated pK_a of the $SDHA^{R451}$ side chain being ~12.0 (*SI Appendix*, Fig. S10 and Table S7). It is therefore tempting to speculate that one role for the capping domain rotation could be in increasing solvent access, tuning the protonation of active site residues, and stabilizing a specific ionization state of $SDHA^{R451}$ or other active site residues during flavinylation.

Impact of Disease-Associated SDHA Mutations on Flavinylation or the Assembly Intermediate. Prior modeling of known disease-associated complex II missense mutations into the structure of assembled porcine complex II did not fully explain why many alterations of the SDHA subunit resulted in complex II insufficiency (3). Thus, we assessed whether it was possible that some of these mutations impacted complex II assembly.

Several complex II missense mutations are almost certainly associated with noncovalent FAD (*SI Appendix*, Fig. S3), for example, $SDHA^{R451C}$ (40) (*SI Appendix*, Fig. S3*A*), where heterozygous mutation is associated with late-onset optic atrophy, ataxia, proximal myopathy, and partial SDH insufficiency (40). The equivalent *E. coli* $SdhA^{R399C}$ showed the protein was devoid of covalent flavin (40) and more conservative substitution of the *E. coli* $FrdA^{R390}$ with Gln or Lys resulted in protein that was similarly unable to support covalent flavinylation (37). The proposal that $SDHA^{R451}$ stabilizes the quinone-methide intermediate explains why covalent flavinylation is eliminated when this side chain is mutated (*SI Appendix*, Fig. S9) (40). In addition, the jugular paraganglioma-associated $SDHA^{H99R}$ (7) (*SI Appendix*, Fig. S3*C*), will prevent covalent flavinylation because the FAD ligand is lost. The equivalent mutation in the *E. coli* complex II (FrdABCD) resulted in a destabilized and totally inactive complex II (21).

We next mapped the locations of other disease-associated SDHA missense mutations onto the SDHA-SDHAF2 assembly intermediate (*SI Appendix*, Fig. S3 and Table S2). While the impact of many of these mutations does not appear to affect this complex, we speculate that the paraganglioma-associated $SDHA^{R589W}$ mutation (48) could impair SDHAF2 binding or complex II assembly. $SDHA^{R589W}$ is located between the flavin-binding domain and the capping domain, and its mutation is anticipated to disrupt the hydrogen bonding that stabilizes the capping domain position in the assembly intermediate (*SI Appendix*, Fig. S3*B*). Consistent with this interpretation, the $SDHA^{R589W}$ mutation has been recapitulated in yeast and shows impairment in the interaction with the assembly factor Sdh5, a complete loss of covalent flavinylation, and an inability to assemble into the mature complex (36).

Discussion

That a flavin could be covalently linked to a protein was first identified in mammalian complex II, with the FAD bound through an 8α-*N*(3)-histidyl-FAD linkage (49, 50) to the SDHA subunit. Subsequently it has been shown that ~10% of all flavoproteins have a covalent flavin linkage (51). A physiological consequence of covalent bond formation is that the redox potential of the flavin cofactor is substantially raised (52). Studies on a variety of covalently flavinylated proteins identify that the increased oxidizing potential imparted by the covalent attachment allows access to more thermodynamically challenging reactions and alters the variety of electron acceptors that can be used by the covalent flavoprotein (21, 51, 53, 54). This is clearly an important protein modification in biology.

Covalent flavin attachment to a polypeptide chain is often proposed as an autocatalytic reaction that requires only apo-protein

and a flavin—the catalytic power of the flavin itself can be harnessed to form the covalent bond (29, 30, 55) through quinone-methide chemistry (41, 42, 51, 54, 56). It is therefore somewhat surprising that complex II requires additional assembly factors for this process (9, 20) (Fig. 1). Perhaps even more surprising is that the SDHAF2 assembly factor has additional functional regions as compared to the close bacterial homolog, SdhE (Fig. 2 *C* and *D* and *SI Appendix*, Fig. S4).

Synthesis of our work here with those in the literature indicate that we have captured the product of the first step in the maturation of the SDHA subunit, which is covalent flavinylation. We also show here that covalent flavinylation of SDHA not only requires the dedicated chaperone SDHAF2, but also a dicarboxylate ligand (Fig. 1). Evaluation of the human SDHA-SDHAF2 structure shows that the synergy between the SDHAF2 assembly factor and the dicarboxylate help to organize the active site of SDHA, which is accomplished by stabilizing the orientation between the flavin-binding domain and the capping domain of the SDHA subunit (*SI Appendix*, Fig. S7 and Tables S4 and S5).

The functional role of the human SDHA-SDHAF2 assembly intermediate has some parallels to the bacterial, yeast, and plant systems (9, 20, 22, 23, 57). Structures for the *E. coli* complex II homologs, FrdA-SdhE and SdhA-SdhE, have been reported (22, 23). Comparison of the human SDHA-SDHAF2 assembly intermediate with the equivalent *E. coli* structures identifies that the SDHAF2/SdhE assembly factors all bind at the same location on the SDHA/FrdA/SdhA flavoprotein (Fig. 2*A*). In each case, this binding location protects a hydrophobic surface from solvent, suggesting classical chaperone activity. Each of these three structures contains a hydrogen bond between a conserved glycine on the assembly factor (human SDHAF2^{G78}, *E. coli* SdhE^{G16}) and the destination ligand for FAD (human SDHA^{H99}, *E. coli* FrdA^{H44}/SdhA^{H45}) that we showed may help orient the ligand and control the electronic state, which may be one way that the assembly factor promotes the flavinylation reaction (Fig. 2*B*) (22, 23). Each structure is associated with the formation of a large, open, and stable channel between solvent and the active site. Our calculations here suggest that this controls the protonation of an active site arginine, SDHA^{R451} in the human protein, with the protonated form predicted to promote the flavinylation reaction by stabilizing the quinone-methide intermediate (*SI Appendix*, Fig. S9) (22, 23). It should be noted that this is solely a result of capping domain rotation in the human enzyme but required the unfolding of several ordered but unstructured loops in the bacterial homologs (*SI Appendix*, Fig. S10) (22, 23). Finally, the domain rotation of each of these structures results in a change in residue presentation at the active site which would disfavor succinate-fumarate interconversion (Fig. 3*D*) (22, 23). Specifically, the alternative active structure induced by the assembly factor displaces a critical threonine residue, human SDHA^{T308}, that stabilizes the transition state between succinate and fumarate (39). In the *E. coli* system, the combination of these findings prompted us to propose that SdhE acts both as classical chaperone and as an alternative accessory subunit of FrdA/SdhA that tunes the enzymatic function of the isolated flavoprotein (22, 23).

Importantly, the two structures of *E. coli* assembly intermediates, i.e., FrdA-SdhE and SdhA-SdhE, were each associated with interdomain rotations that differed both in magnitude and in the rotation axis (*SI Appendix*, Fig. S6 *C* and *D*) (22, 23). This caused some controversy because the structure of the *E. coli* FrdA-SdhE required a cross-linker to stabilize the complex (22), while the *E. coli* SdhA-SdhE did not require a cross-linker but lacked bound dicarboxylate (23) (*SI Appendix*, Table S5). We find that the pose of human SDHA-SDHAF2 more strongly resembles the interdomain orientation observed in the cross-linked *E. coli* FrdA-SdhE assembly intermediate, which contained malonate at the active site (*SI Appendix*, Fig. S11) (22). Specifically, the capping domains rotate along more similar axes, albeit to somewhat different magnitudes (~11° versus ~25°). In contrast, the domain movement of the *E. coli* SdhA-SdhE lacking dicarboxylate is along a substantially different rotation axis and undergoes a much larger rotation of >40° to a more open state (23). As a note, each of these structures has two copies of the protein complex in the asymmetric unit, with the interdomain rotation being close to the same in each copy.

Consideration of all of the states and conditions from SDHA homologs in reported structures (23, 34, 58) identifies that the flavin-binding domain and capping-domain exhibit four reported interdomain orientations that may represent different functional states. First, there is a close set of defined interdomain orientations associated with the mature catalytic form (Fig. 4*A*) (5, 34, 44–46, 59). As discussed extensively in the literature, this form optimizes the active site for the interconversion of fumarate and succinate (5, 34, 44–46, 59). Most critically, this involves aligning an arginine (human SDHA^{R340}) to allow proton shuttling to or from the substrate (24, 59, 60) and allowing a threonine (SDHA^{T308}) to stabilize the transition state (39). Second, there is a similar set of interdomain positions in the flavinylation product form, which contains the flavoprotein, the assembly factor, and an essential dicarboxylate cofactor. We observe this in the structures of both human SDHA-SDHAF2 with oxaloacetate and in *E. coli* FrdA-SdhE with malonate (Fig. 4*B*) (22). Importantly, the interdomain orientation observed in these two structures is stabilized by the dicarboxylate (Fig. 1 and *SI Appendix*, Fig. S11). The flavinylation product form may disfavor succinate-fumarate interconversion by altering the arrangement of catalytically important residues including the SDHA^{R340} proton shuttle and the SDHA^{T308} side chain that stabilizes the transition state of succinate-fumarate interconversion (39). While the flavinylation form is relatively closed, the orientation between the capping domain and flavin domain site is distinct from the catalytic form. At the same time, solvent access to SDHA^{R451} likely affects the side chain pK_a in order to stabilize the quinone-methide intermediate. The third form is an open form, which was observed in the *E. coli* SdhA-SdhE structure without the essential dicarboxylate cofactor (23) (Fig. 4*C* and *SI Appendix*, Fig. S11). This form shares some key structural features with the flavinylation product form. Specifically, the active site of this structure is not aligned for succinate-fumarate interconversion and there is solvent access to the active site arginine, which affects its calculated pK_a. Although these are the currently understood mechanistic requirements for promoting covalent flavinylation and disfavoring succinate-fumarate interconversion, the lack of the dicarboxylate cofactor suggests that this form is not functional for flavinylation. The capping domain rotates away from the flavin domain along a different axis than is observed in the flavinylation form and the rotation is of much larger magnitude. Its position in the structure is stabilized by numerous intradomain hydrogen bonds to the flavin-binding domain. Indeed, this *E. coli* SdhA-SdhE structure has substantially more buried surface area than the *E. coli* FrdA-SdhE and was stable during size exclusion chromatography (23). One possibility is that structure may be poised to interact with SdhB; alternatively, it may be an off-pathway pose. Further experiments are necessary to clarify the mechanistic role of the dicarboxylate in order to distinguish between these possibilities. Finally, an apo form subunit has been observed in the structure of the noncovalent FAD *E. coli* homolog L-aspartate oxidase (Fig. 4*D*) (58). Here, a very large interdomain rotation stabilizes a large tunnel to the active site, which would allow FAD insertion (58).

A major difference between the human SDHA-SDHAF2 structure and the previously reported bacterial structures (22, 23) is the extensive buried surface area in the human system, which makes the assembly intermediate highly stable (Fig. 2*A*). One interpretation of this enhanced stability is that the isolated and unassembled human SDHA is either more unstable, more

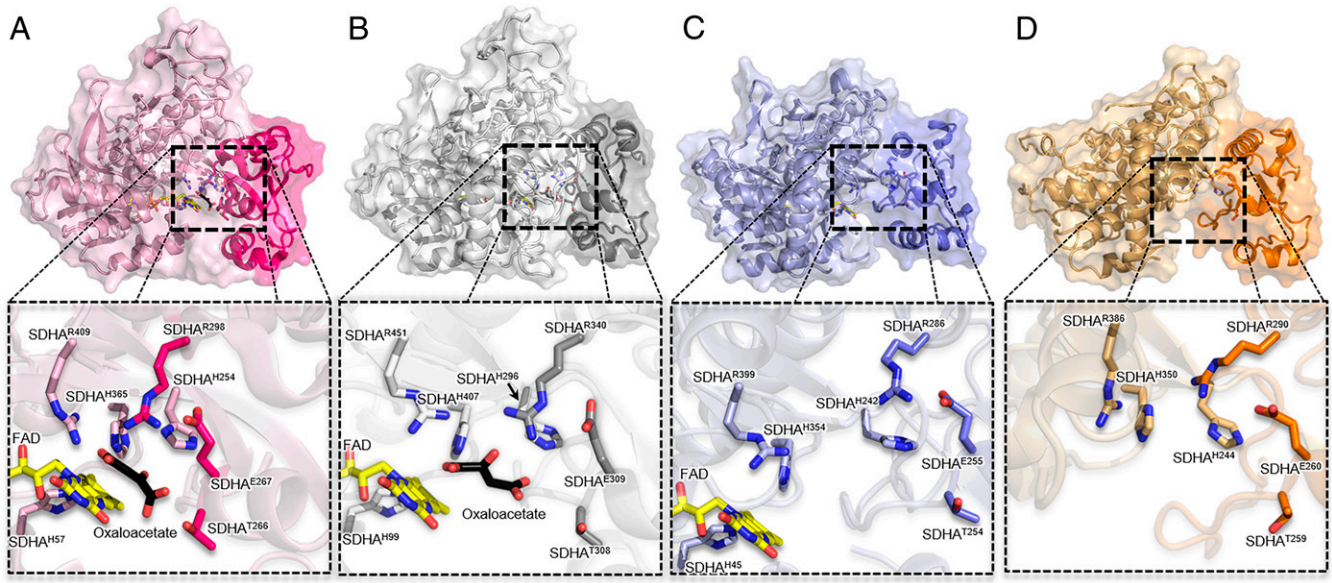

Fig. 4. Different catalytic forms of SDHA orthologs. (*A*) The catalytic form has a closed interdomain orientation that optimizes the active site for the interconversion of succinate and fumarate. It has been observed in structures of assembled bacterial and mitochondrial complex II (34, 44–46) and is exemplified here by assembled porcine complex II (PDB ID 3SFD) (34). (*B*) The flavinylation product form, is hallmarked by the rotation of the capping domain, which in turn alters the alignment of active site residues and disfavors succinate-fumarate conversion (22, 23). This form also has ready solvent access to an active site arginine (equivalent to $SDHA^{R451}$) and contains an essential dicarboxylate cofactor bound in a position distinct from that observed in the catalytic form of the assembled enzyme. The flavinylation product form has been observed in the human SDHA-SDHAF2 assembly intermediate and the *E. coli* FrdA-SdhE assembly intermediate (PDB ID 6B58) (22) and is represented by the human SDHA-SDHAF2 assembly intermediate here. (*C*) The open form contains many of the hallmarks of the flavinylation product form, including a misaligned active site and solvent access to an active site arginine. The capping domain rotation is along a different axis and is of much larger magnitude, and this form lacks the dicarboxylate cofactor necessary for the covalent flavinylation reaction. To date, this form has only been observed in *E. coli* SDHA-SdhE assembly intermediate (PDB ID 6C12) (23), which is shown here. (*D*) The apo form, contains the largest interdomain rotation and lacks bound FAD, thus it is catalytically incompetent. The apo form has only been observed in the structure of the *E. coli* L-aspartate oxidase (PDB ID 1CHU) (58).

aggregation prone, and/or more deleterious to cellular function and therefore SDHAF2 evolved to have a more stringent chaperone function. Indeed, one confirmed role for SDHAF2 is in protecting SDHA from proteolysis (12) which would be consistent with free SDHA being unstable in the mitochondrial matrix. Another possibility is suggested by prior reports from the J. Neuzil laboratory, which identify the accumulation of an alternative low molecular weight form of complex II, termed CII_{low} (19). CII_{low} was proposed as a storage form of complex II during periods of bioenergetic stress that is used to control metabolic balance. Mass spectrometry of CII_{low} purified from mitochondria identified the presence of SDHA, SDHAF2, and SDHAF4 (19). Given the molecular weight of CII_{low}, this could include the very stable SDHA-SDHAF2 complex that we identify here. A stable matrix-localized intermediate like SDHA-SDHAF2 (19) may also contribute to the mitochondrial signaling cascade that is important for bioenergetic balance (61). While the additional biological roles of CII_{low} are continuing to be explored, any human mutations that affect the ability of SDHA to bind to SDHAF2 (*SI Appendix*, Fig. S3) could disrupt other functions of CII_{low} and therefore have physiological impacts beyond complex II insufficiency. This may partially explain the broad range of distinct disease presentations in patients with missense mutations of complex II (*SI Appendix*, Table S2) (3, 7–9, 40, 48, 62–67).

In summary, we provide a view of the covalent flavinylation reaction catalyzed by the human SDHA subunit. This pose may represent the product of the first step in what is anticipated to be a multistep process of maturation in an integral-membrane complex that contains four subunits, covalent flavin, three distinct Fe-S clusters, and *b*-type heme. Additional work is needed to reveal the essential mechanistic role of the dicarboxylate in flavinylation and how SDHAF2 is displaced from this intermediate in order to proceed through the remaining steps of complex II maturation. In addition, future studies may focus on the maturation of other subunits within this complex.

Materials and Methods

In vitro flavinylation of purified apo-SDHA was performed in the presence of 25 μM FAD and 20 mM of the indicated dicarboxylate at 37 °C for 40 min. Proteins were separated by SDS/PAGE (polyacrylamide gel electrophoresis) and the gel was incubated in 10% acetic acid/20% ethanol for 5 min. In-gel fluorescence of covalently attached FAD was detected using ultraviolet (UV) fluorescence. The gel then was rinsed with water for 5 min and stained to assess total protein. Band intensities were quantified with ImageJ (NIH) software.

Crystallization was performed at room temperature via the hanging drop vapor diffusion method by mixing 15 mg/mL of purified SDHA-SDHAF2 (in 20 mM Hepes pH 7.5) in a 1:1 ratio with reservoir solution (100 mM sodium malonate pH 5.0 and 12% polyethylene glycol [PEG] 3350). Diffraction data were collected at the Advanced Photon Source using the Life Sciences Collaborative Access Team (LS-CAT) beamlines. The structure was determined by molecular replacement using the SDHA subunit of porcine complex II as the search model (PDB ID 1ZOY ref. 34). Data collection and refinement statistics are listed in *SI Appendix*, Table S2.

Detailed information on the constructs developed, procedures for the expression and purification of SDHA and SDHAF2, crystallization of the assembly intermediate, and all kinetic and biochemical measurements are described in *SI Appendix, Materials and Methods*.

Protein Numbering Scheme. There are two distinct numbering schemes for mitochondrial SDHA and SDHAF2 used in the literature. These schemes depend upon whether the numbering begins with the mitochondrial signal sequence or whether it begins with the N-terminal residue of the mature protein. In published structures of avian and porcine mitochondrial complex II proteins, numbering began with the N terminus of the mature protein. Here, we followed the numbering scheme that is used in the majority of the literature describing patient mutations, which is numbered from the beginning of the

mitochondrial signaling sequence of both SDHA and SDHAF2 (*SI Appendix*, Table S1).

Data Availability. PDB coordinates and processed diffraction data have been deposited in the Protein Data Bank with accession code 6VAX (details in *SI Appendix*, Table S2) (31). Raw diffraction data have been deposited with SBGrid (DOI: 10.15785/SBGRID/748) with accession code 748 (32). Raw gel images used in Fig. 1 are available by request from gary.cecchini@ucsf.edu.

ACKNOWLEDGMENTS. We thank Dr. Srinivas Chakravarthy and all Advanced Photon Source (APS)-Biophysics Collaborative Access Team (BioCAT) beamline staff for assistance with SEC-SAXS data collection and Rupesh Agarwal for assistance in pKa calculations. This research used resources of the Advanced Photon Source, a Department of Energy (DOE) Office of Science User Facility operated for the DOE Office of Science by the Argonne National Laboratory under Contract DE-AC02-06CH11357. Use of the LS-CAT Sector 21 was supported by the Michigan Economic Development Corporation and the Michigan Technology Tri-Corridor (Grant 085P1000817). Use of the Advanced Photon Source was supported by the the DOE Office of Basic Energy Sciences, under Contract DE-AC02-06CH11357. This work was supported by NIH Award GM61606. G.C. is the recipient of Senior Research Career Scientist Award 1K6B004215 from the Department of Veterans Affairs. P.S. is supported by Postdoctoral Fellowship 19POST34450093 from the American Heart Association.

1. V. Yankovskaya *et al*., Architecture of succinate dehydrogenase and reactive oxygen species generation. *Science* **299**, 700–704 (2003).
2. F. Sun *et al*., Crystal structure of mitochondrial respiratory membrane protein complex II. *Cell* **121**, 1043–1057 (2005).
3. T. M. Iverson, E. Maklashina, G. Cecchini, Structural basis for malfunction in complex II. *J. Biol. Chem.* **287**, 35430–35438 (2012).
4. T. M. Iverson, Catalytic mechanisms of complex II enzymes: A structural perspective. *Biochim. Biophys. Acta* **1827**, 648–657 (2013).
5. G. Cecchini, Function and structure of complex II of the respiratory chain. *Annu. Rev. Biochem.* **72**, 77–109 (2003).
6. C. Hägerhäll, Succinate: quinone oxidoreductases. Variations on a conserved theme. *Biochim. Biophys. Acta* **1320**, 107–141 (1997).
7. B. Bausch *et al*.; European-American-Asian Pheochromocytoma-Paraganglioma Registry Study Group, Clinical characterization of the pheochromocytoma and paraganglioma susceptibility genes SDHA, TMEM127, MAX, and SDHAF2 for gene-informed prevention. *JAMA Oncol.* **3**, 1204–1212 (2017).
8. B. A. Ackrell, Cytopathies involving mitochondrial complex II. *Mol. Aspects Med.* **23**, 369–384 (2002).
9. H. X. Hao *et al*., SDH5, a gene required for flavination of succinate dehydrogenase, is mutated in paraganglioma. *Science* **325**, 1139–1142 (2009).
10. J. Rutter, D. R. Winge, J. D. Schiffman, Succinate dehydrogenase–Assembly, regulation and role in human disease. *Mitochondrion* **10**, 393–401 (2010).
11. J. G. Van Vranken *et al*., SDHAF4 promotes mitochondrial succinate dehydrogenase activity and prevents neurodegeneration. *Cell Metab.* **20**, 241–252 (2014).
12. A. Bezawork-Geleta, T. Saiyed, D. A. Dougan, K. N. Truscott, Mitochondrial matrix proteostasis is linked to hereditary paraganglioma: LON-mediated turnover of the human flavinylation factor SDH5 is regulated by its interaction with SDHA. *FASEB J.* **28**, 1794–1804 (2014).
13. K. Belt, O. Van Aken, M. Murcha, A. H. Millar, S. Huang, An assembly factor promotes assembly of flavinated SDH1 into the succinate dehydrogenase complex. *Plant Physiol.* **177**, 1439–1452 (2018).
14. B. Moosavi, E. A. Berry, X. L. Zhu, W. C. Yang, G. F. Yang, The assembly of succinate dehydrogenase: A key enzyme in bioenergetics. *Cell. Mol. Life Sci.* **76**, 4023–4042 (2019).
15. D. Ghezzi *et al*., SDHAF1, encoding a LYR complex-II specific assembly factor, is mutated in SDH-defective infantile leukoencephalopathy. *Nat. Genet.* **41**, 654–656 (2009).
16. N. Maio *et al*., Disease-causing SDHAF1 mutations impair transfer of Fe-S clusters to SDHB. *Cell Metab.* **23**, 292–302 (2016).
17. U. Na *et al*., The LYR factors SDHAF1 and SDHAF3 mediate maturation of the iron-sulfur subunit of succinate dehydrogenase. *Cell Metab.* **20**, 253–266 (2014).
18. K. I. Wolf *et al*., A family with a carotid body paraganglioma and thyroid neoplasias with a new *SDHAF2* germline variant. *J. Endocr. Soc.* **3**, 2151–2157 (2019).
19. A. Bezawork-Geleta *et al*., Alternative assembly of respiratory complex II connects energy stress to metabolic checkpoints. *Nat. Commun.* **9**, 2221 (2018).
20. M. B. McNeil, J. S. Clulow, N. M. Wilf, G. P. Salmond, P. C. Fineran, SdhE is a conserved protein required for flavinylation of succinate dehydrogenase in bacteria. *J. Biol. Chem.* **287**, 18418–18428 (2012).
21. M. Blaut *et al*., Fumarate reductase mutants of Escherichia coli that lack covalently bound flavin. *J. Biol. Chem.* **264**, 13599–13604 (1989).
22. P. Sharma, E. Maklashina, G. Cecchini, T. M. Iverson, Crystal structure of an assembly intermediate of respiratory complex II. *Nat. Commun.* **9**, 274 (2018).
23. M. J. Maher, A. S. Herath, S. R. Udagedara, D. A. Dougan, K. N. Truscott, Crystal structure of bacterial succinate:quinone oxidoreductase flavoprotein SdhA in complex with its assembly factor SdhE. *Proc. Natl. Acad. Sci. U.S.A.* **115**, 2982–2987 (2018).
24. E. Maklashina, S. Rajagukguk, T. M. Iverson, G. Cecchini, The unassembled flavoprotein subunits of human and bacterial complex II have impaired catalytic activity and generate only minor amounts of ROS. *J. Biol. Chem.* **293**, 7754–7765 (2018).
25. L. Zafreen, N. Walker-Kopp, L. S. Huang, E. Berry, In-vitro, SDH5-dependent flavinylation of immobilized human respiratory complex II flavoprotein. *Arch. Biochem. Biophys.* **604**, 47–56 (2016).
26. K. A. Davis, Y. Hatefi, Succinate dehydrogenase. I. Purification, molecular properties, and substructure. *Biochemistry* **10**, 2509–2516 (1971).
27. R. Brandsch, V. Bichler, Covalent cofactor binding to flavoenzymes requires specific effectors. *Eur. J. Biochem.* **182**, 125–128 (1989).
28. A. Kounosu, Analysis of covalent flavinylation using thermostable succinate dehydrogenase from Thermus thermophilus and Sulfolobus tokodaii lacking SdhE homologs. *FEBS Lett.* **588**, 1058–1063 (2014).
29. A. Hassan-Abdallah, R. C. Bruckner, G. Zhao, M. S. Jorns, Biosynthesis of covalently bound flavin: Isolation and in vitro flavinylation of the monomeric sarcosine oxidase apoprotein. *Biochemistry* **44**, 6452–6462 (2005).
30. J. Jin *et al*., Covalent flavinylation of vanillyl-alcohol oxidase is an autocatalytic process. *FEBS J.* **275**, 5191–5200 (2008).
31. P. Sharma, E. Maklashina, G. Cecchini, T. M. Iverson, Crystal structure of human SDHA-ADHAF2 assembly intermediate. Protein Data Bank. https://doi.org/10.2210/pdb6VAX/pdb. Deposited 18 December 2019.
32. P. Sharma, E. Maklashina, G. Cecchini, T. M. Iverson, X-Ray Diffraction data from Human SDHA-SDHAF2 complex, source of 6VAX structure. SBGrid. DOI: 10.15785/SBGRID/748. Deposited 18 December 2019.
33. A. Eletsky *et al*., Solution NMR structure of yeast succinate dehydrogenase flavinylation factor Sdh5 reveals a putative Sdh1 binding site. *Biochemistry* **51**, 8475–8477 (2012).
34. Q. Zhou *et al*., Thiabendazole inhibits ubiquinone reduction activity of mitochondrial respiratory complex II via a water molecule mediated binding feature. *Protein Cell* **2**, 531–542 (2011).
35. G. Qi, R. Lee, S. Hayward, A comprehensive and non-redundant database of protein domain movements. *Bioinformatics* **21**, 2832–2838 (2005).
36. H. J. Kim, M. Y. Jeong, U. Na, D. R. Winge, Flavinylation and assembly of succinate dehydrogenase are dependent on the C-terminal tail of the flavoprotein subunit. *J. Biol. Chem.* **287**, 40670–40679 (2012).
37. C. A. Starbird *et al*., Structural and biochemical analyses reveal insights into covalent flavinylation of the *Escherichia coli* complex II homolog quinol:fumarate reductase. *J. Biol. Chem.* **292**, 12921–12933 (2017).
38. V. W. Cheng *et al*., Redox state of flavin adenine dinucleotide drives substrate binding and product release in Escherichia coli succinate dehydrogenase. *Biochemistry* **54**, 1043–1052 (2015).
39. T. M. Tomasiak, E. Maklashina, G. Cecchini, T. M. Iverson, A threonine on the active site loop controls transition state formation in Escherichia coli respiratory complex II. *J. Biol. Chem.* **283**, 15460–15468 (2008).
40. M. A. Birch-Machin, R. W. Taylor, B. Cochran, B. A. Ackrell, D. M. Turnbull, Late-onset optic atrophy, ataxia, and myopathy associated with a mutation of a complex II gene. *Ann. Neurol.* **48**, 330–335 (2000).
41. M. Mewies, W. S. McIntire, N. S. Scrutton, Covalent attachment of flavin adenine dinucleotide (FAD) and flavin mononucleotide (FMN) to enzymes: The current state of affairs. *Protein Sci.* **7**, 7–20 (1998).
42. C. Walsh, Flavin coenzymes: At the crossroads of biological redox chemistry. *Acc. Chem. Res.* **13**, 148–155 (1980).
43. P. Sharma, E. Maklashina, G. Cecchini, T. M. Iverson, Maturation of the respiratory complex II flavoprotein. *Curr. Opin. Struct. Biol.* **59**, 38–46 (2019).
44. L. S. Huang, J. T. Shen, A. C. Wang, E. A. Berry, Crystallographic studies of the binding of ligands to the dicarboxylate site of complex II, and the identity of the ligand in the "oxaloacetate-inhibited" state. *Biochim. Biophys. Acta* **1757**, 1073–1083 (2006).
45. J. Ruprecht, V. Yankovskaya, E. Maklashina, S. Iwata, G. Cecchini, Structure of Escherichia coli succinate:quinone oxidoreductase with an occupied and empty quinone-binding site. *J. Biol. Chem.* **284**, 29836–29846 (2009).
46. T. M. Tomasiak *et al*., Geometric restraint drives on- and off-pathway catalysis by the Escherichia coli menaquinol:fumarate reductase. *J. Biol. Chem.* **286**, 3047–3056 (2011).
47. T. M. Iverson, C. Luna-Chavez, G. Cecchini, D. C. Rees, Structure of the Escherichia coli fumarate reductase respiratory complex. *Science* **284**, 1961–1966 (1999).
48. N. Burnichon *et al*., SDHA is a tumor suppressor gene causing paraganglioma. *Hum. Mol. Genet.* **19**, 3011–3020 (2010).
49. E. B. Kearney, Studies on succinic dehydrogenase. XII. Flavin component of the mammalian enzyme. *J. Biol. Chem.* **235**, 865–877 (1960).
50. J. Salach *et al*., Studies on succinate dehydrogenase. Site of attachment of the covalently-bound flavin to the peptide chain. *Eur. J. Biochem.* **26**, 267–278 (1972).
51. D. P. Heuts, N. S. Scrutton, W. S. McIntire, M. W. Fraaije, What's in a covalent bond? On the role and formation of covalently bound flavin cofactors. *FEBS J.* **276**, 3405–3427 (2009).
52. D. E. Edmondson, T. P. Singer, Oxidation-reduction properties of the 8 alpha-substituted flavins. *J. Biol. Chem.* **248**, 8144–8149 (1973).
53. M. W. Fraaije, R. H. van den Heuvel, W. J. van Berkel, A. Mattevi, Covalent flavinylation is essential for efficient redox catalysis in vanillyl-alcohol oxidase. *J. Biol. Chem.* **274**, 35514–35520 (1999).
54. D. E. Edmondson, P. Newton-Vinson, The covalent FAD of monoamine oxidase: Structural and functional role and mechanism of the flavinylation reaction. *Antioxid. Redox Signal.* **3**, 789–806 (2001).

55. R. Brandsch, V. Bichler, Autoflavinylation of apo6-hydroxy-D-nicotine oxidase. *J. Biol. Chem.* **266**, 19056–19062 (1991).
56. J. W. Frost, W. H. Rastetter, Biomimetic 8α functionalization of riboflavin. *J. Am. Chem. Soc.* **102**, 7157–7159 (1980).
57. S. Huang, N. L. Taylor, E. Ströher, R. Fenske, A. H. Millar, Succinate dehydrogenase assembly factor 2 is needed for assembly and activity of mitochondrial complex II and for normal root elongation in Arabidopsis. *Plant J.* **73**, 429–441 (2013).
58. A. Mattevi *et al*., Structure of L-aspartate oxidase: Implications for the succinate dehydrogenase/fumarate reductase oxidoreductase family. *Structure* **7**, 745–756 (1999).
59. E. Maklashina *et al*., Fumarate reductase and succinate oxidase activity of Escherichia coli complex II homologs are perturbed differently by mutation of the flavin binding domain. *J. Biol. Chem.* **281**, 11357–11365 (2006).
60. K. L. Pankhurst *et al*., A proton delivery pathway in the soluble fumarate reductase from Shewanella frigidimarina. *J. Biol. Chem.* **281**, 20589–20597 (2006).
61. T. Finkel, Signal transduction by mitochondrial oxidants. *J. Biol. Chem.* **287**, 4434–4440 (2012).
62. T. Bourgeron *et al*., Mutation of a nuclear succinate dehydrogenase gene results in mitochondrial respiratory chain deficiency. *Nat. Genet.* **11**, 144–149 (1995).
63. R. Horváth *et al*., Leigh syndrome caused by mutations in the flavoprotein (Fp) subunit of succinate dehydrogenase (SDHA). *J. Neurol. Neurosurg. Psychiatry* **77**, 74–76 (2006).
64. A. Levitas *et al*., Familial neonatal isolated cardiomyopathy caused by a mutation in the flavoprotein subunit of succinate dehydrogenase. *Eur. J. Hum. Genet.* **18**, 1160–1165 (2010).
65. A. T. Pagnamenta *et al*., Phenotypic variability of mitochondrial disease caused by a nuclear mutation in complex II. *Mol. Genet. Metab.* **89**, 214–221 (2006).
66. B. Parfait *et al*., Compound heterozygous mutations in the flavoprotein gene of the respiratory chain complex II in a patient with Leigh syndrome. *Hum. Genet.* **106**, 236–243 (2000).
67. R. Van Coster *et al*., Homozygous Gly555Glu mutation in the nuclear-encoded 70 kDa flavoprotein gene causes instability of the respiratory chain complex II. *Am. J. Med. Genet. A.* **120A**, 13–18 (2003).